

## Magnetism of Cr in V/Cr multilayers studied by $^{119}\text{Sn}$ Mössbauer spectroscopy

This article has been downloaded from IOPscience. Please scroll down to see the full text article.

2000 J. Phys.: Condens. Matter 12 9247

(<http://iopscience.iop.org/0953-8984/12/44/307>)

View [the table of contents for this issue](#), or go to the [journal homepage](#) for more

Download details:

IP Address: 171.66.16.221

The article was downloaded on 16/05/2010 at 06:56

Please note that [terms and conditions apply](#).

## Magnetism of Cr in V/Cr multilayers studied by $^{119}\text{Sn}$ Mössbauer spectroscopy

M Almokhtar<sup>†</sup>, K Mibu<sup>†</sup>, A Nakanishi<sup>‡</sup>, T Kobayashi<sup>‡</sup> and T Shinjo<sup>†</sup>

<sup>†</sup> Institute for Chemical Research, Kyoto University, Uji, Kyoto-fu 611-0011, Japan

<sup>‡</sup> Department of Physics, Shiga University of Medical Science, Otsu Shiga 520-2192, Japan

Received 18 July 2000, in final form 15 September 2000

**Abstract.** The magnetic properties of thin Cr layers in epitaxial V/Cr multilayered structures were investigated at room temperature and 15 K via  $^{119}\text{Sn}$  Mössbauer spectroscopy. The magnetic moment and the Néel temperature of Cr, as inferred from the magnetic hyperfine fields transferred to the  $^{119}\text{Sn}$  monatomic layers inserted in Cr layers, were found to reduce on decreasing the Cr layer thickness below 40 Å. The local magnetic structure along the growth direction of 80 Å thick Cr layers was investigated by changing the Sn probe positions. The effect of the V/Cr interface on the Cr magnetism is discussed.

### 1. Introduction

The unique nature of the itinerant antiferromagnetism and the spin-density-wave (SDW) magnetic structure in Cr have attracted intensive investigation during the last few decades [1]. In layered structures, the magnetic properties of thin Cr films change drastically due to dimensional and boundary effects such as: broken symmetry along the growth direction, hybridization at the interface and proximity with ferromagnetic or paramagnetic boundary layers [2, 3]. For Fe/Cr multilayers with ideally flat interfaces, the magnetic exchange coupling at the Fe/Cr interface is thought to stabilize the magnetic ordered state of very thin Cr layers at temperatures higher than its bulk Néel temperature [3–7]. However, the role of the magnetic exchange coupling at the Fe/Cr interface in the magnetic state of thin Cr layers is still an open question. The results obtained by perturbed angular correlation (PAC) measurements on both Fe/Cr and Ag/Cr multilayers show that the SDW collapses and Cr becomes non-magnetic below a critical thickness of 60 Å, which is comparable with the SDW period [8]. At such small thickness, neutron scattering investigations cannot distinguish whether Cr atoms in Fe/Cr multilayers have reduced magnetic moments or are ordered as inhomogeneous AF domains which result in a small average magnetic moment [9]. In this paper, epitaxial multilayered structures of V/Cr are studied to clarify the magnetic properties of Cr layers confined by paramagnetic boundary layers. In this case no ferromagnetic proximity effect occurs at the interface and a suppression of the Cr magnetic moments due to the hybridization between the d-band electrons of V and Cr is expected.

Non-magnetic Sn has been used as a probe to study the local magnetism of bulk Cr and its alloys via Mössbauer spectroscopy [10]. The magnitude and direction of Cr magnetic moments can be inferred from the magnitude and the orientation of the hyperfine fields transferred at the Sn nuclear sites. For layered structures, Sn was found to grow epitaxially with bcc Cr(001) on an MgO(001) substrate [11]. A large hyperfine field around 12 T was reported at the nuclear

sites of Sn monatomic layers embedded in bcc Cr(001) layers. A reduction of the Cr magnetic moment with reducing Cr layer thickness was reported for Fe/Cr/Sn/Cr multilayers where Cr/Sn/Cr is sandwiched with Fe [12].

## 2. Experimental procedure

$[V(10 \text{ \AA})/Cr(t \text{ \AA})/Sn(2 \text{ \AA})/Cr(t \text{ \AA})]_{\times 29}/V(10 \text{ \AA})$  multilayered structures were epitaxially grown on MgO(001) substrates kept at room temperature and 200 °C using an ultrahigh-vacuum deposition technique with electron-gun heating. The thickness of the V layers was fixed at 10 Å and the Cr layer thickness between V layers,  $t_{Cr} = 2t$ , was changed from 10 Å to 80 Å. A Cr (50 Å) buffer layer was deposited at 200 °C on the MgO (001) substrate prior to the multilayer growth for both growth temperatures. The deposition rate was set around 0.3 Å s<sup>-1</sup> and the pressure was in the 10<sup>-9</sup> Torr range. Another series of multilayered structures designated as MgO (001)/Cr(50 Å)/ $[V(10 \text{ \AA})/Cr(80 - t \text{ \AA})/Sn(2 \text{ \AA})/Cr(t \text{ \AA})]_{\times 29}/V(10 \text{ \AA})$ , where  $t_{Cr} = 80 \text{ \AA}$  and  $t = 5, 10, 20, 40, 60, 70, 75 \text{ \AA}$ , were grown by the same growth procedures. The epitaxial growth of Cr and V layers in the bcc (001) direction was characterized by x-ray diffraction (XRD) in both high- and low-angle regions using Cu K $\alpha$  radiation. The in-plane lattice spacing was investigated through off-axis XRD scans around the bcc Cr(112) peak. The local magnetic properties around the Sn layers were examined through <sup>119</sup>Sn conversion-electron Mössbauer spectroscopy (CEMS) using a Ca<sup>119m</sup>SnO<sub>3</sub>  $\gamma$ -ray source and a He + 1%(CH<sub>3</sub>)<sub>3</sub>CH gas-flow counter at room temperature and a H<sub>2</sub> gas-filled counter at 15 K [13]. The direction of the incident  $\gamma$ -rays was set parallel to the film normal.

## 3. Results and discussion

### 3.1. Structural characterization

Bulk vanadium has a bcc structure with a lattice constant ( $a_V = 3.03 \text{ \AA}$ ) larger than that of bcc Cr ( $a_{Cr} = 2.88 \text{ \AA}$ ) by 5.2%. The high-angle XRD measurements in a  $\theta$ -2 $\theta$  scan with the scattering vector normal to the film plane for samples deposited at 200 °C are shown in figure 1. The observed V/Cr (002) fundamental peak with superlattice satellite reflections indicates that both V and Cr grow epitaxially with the [001] direction perpendicular to the film plane and that the artificial periodicity is well established through the samples. The (002) peak resulting from both Cu K $\alpha_1$  and Cu K $\alpha_2$  radiation could be distinguished for all the samples prepared, indicating the high structural coherence in the growth direction. The modulation period length estimated from the positions of satellite peaks using the relation  $\Lambda = 2\pi/\delta Q$ , where  $\delta Q$  is the average spacing between  $Q$ -values ( $Q = 4\pi(\sin \theta)/\lambda$ ), agrees well with the designed period. The rocking curves around the (002) peaks revealed a full width at half-maximum (FWHM) around 1° for all the samples, confirming the high degree of the crystalline orientation.

The low-angle x-ray patterns as well as the periods determined from the peak positions are shown in figure 2. Superlattice reflections resulting from the chemical modulation were observed up to the fifth order for  $[V(10 \text{ \AA})/Cr(40 \text{ \AA})/Sn(2 \text{ \AA})/Cr(40 \text{ \AA})]_{\times 29}/V(10 \text{ \AA})$ . The short-period oscillations observed for  $[V(10 \text{ \AA})/Cr(5 \text{ \AA})/Sn(2 \text{ \AA})/Cr(5 \text{ \AA})]_{\times 29}/V(10 \text{ \AA})$  result from the total film thickness and indicate the smoothness of the film surface. The features of the diffraction patterns indicate that the layers are smooth and have defined interfaces. The x-ray diffraction patterns for the samples deposited at room temperature in both low- and high-angle regions show almost the same features as those of the samples deposited at 200 °C. This feature indicates that neither epitaxy nor interface structure change especially remarkably on increasing the growth temperature up to 200 °C. The structural relation in the film plane is

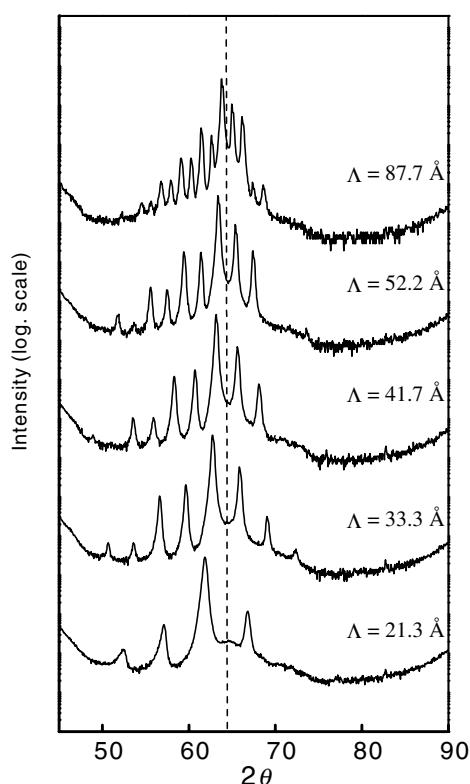


**Figure 1.** X-ray diffraction patterns in the high-angle region for the multilayer structure  $[V(10 \text{ \AA})/Cr(t \text{ \AA})/Sn(2 \text{ \AA})/Cr(t \text{ \AA})]_{\times 29}/V(10 \text{ \AA})$  for  $t = 5, 10, 15, 20, 40 \text{ \AA}$  (from the bottom to the top). The estimated multilayer period is shown. The dashed line refers to the position of the (002) peak for bulk Cr.

$MgO[100] \parallel Cr[110] \parallel V[110]$ . The estimated in-plane (110) lattice constant is larger than that of bulk Cr by about 1.6% for  $[V(10 \text{ \AA})/Cr(10 \text{ \AA})/Sn(2 \text{ \AA})/Cr(10 \text{ \AA})]_{\times 29}/V(10 \text{ \AA})$ .

### 3.2. Mössbauer spectroscopy

The magnetic properties of Cr layers investigated by means of Mössbauer spectroscopic measurements are discussed in three sections. In the first section, the dependence of the hyperfine field on the thickness of the Cr layers ( $t_{Cr}$ ) bounded by V is considered. Here, a monatomic Sn layer is located at the middle of the Cr layers with the multilayer structure  $[V(10 \text{ \AA})/Cr(t \text{ \AA})/Sn(2 \text{ \AA})/Cr(t \text{ \AA})]_{\times 29}/V(10 \text{ \AA})$ , where  $t = t_{Cr}/2$ . The second section shows the Mössbauer measurements performed at 15 K to characterize the Cr magnetic properties at low temperatures. In the third section, the Cr magnetic structures at different positions in the direction perpendicular to the film plane are investigated using the multilayered structures  $[V(10 \text{ \AA})/Cr(80 - t \text{ \AA})/Sn(2 \text{ \AA})/Cr(t \text{ \AA})]_{\times 29}/V(10 \text{ \AA})$ , where  $t_{Cr} = 80 \text{ \AA}$  and  $t = 5, 10, 20, 40, 60, 70, 75 \text{ \AA}$ . The effect of the V/Cr interface is discussed.

**3.2.1. The dependence of the Cr magnetization on the Cr layer thickness.** The spectra collected at room temperature for the samples deposited at 200 °C with the multilayer

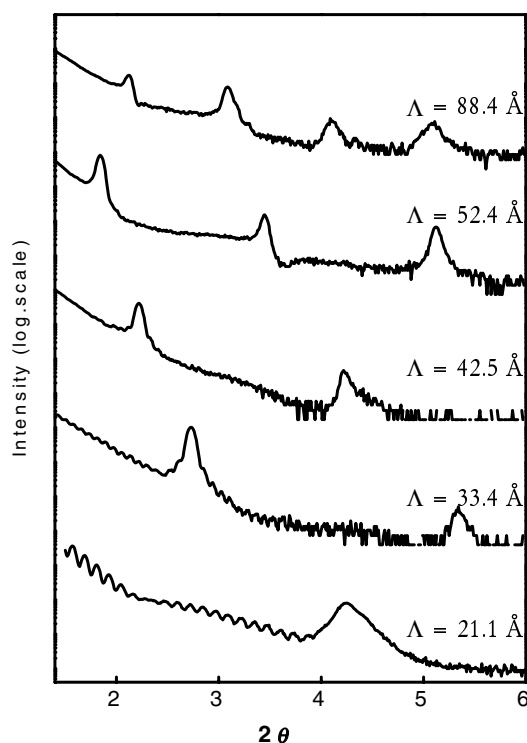


**Figure 2.** X-ray diffraction patterns in the low-angle region for the multilayer structure  $[V(10 \text{ \AA})/Cr(t \text{ \AA})/Sn(2 \text{ \AA})/Cr(t \text{ \AA})]_{\times 29}/V(10 \text{ \AA})$  for  $t = 5, 10, 15, 20, 40 \text{ \AA}$  (from the bottom to the top). The estimated multilayer period is shown.

structures  $[V(10 \text{ \AA})/Cr(t \text{ \AA})/Sn(2 \text{ \AA})/Cr(t \text{ \AA})]_{\times 29}/V(10 \text{ \AA})$ , where  $t = 40, 20, 15, 10, 5 \text{ \AA}$ , are shown in figure 3. The isomer shift (relative to  $CaSnO_3$ ) obtained from fitting the spectra is  $1.56 \pm 0.2 \text{ mm s}^{-1}$ . This value is almost the same as that reported for Sn dissolved in Cr [10]. The best fit for all the spectra was obtained when the angle of the hyperfine field was set to  $10 \pm 5^\circ$  relative to the film normal. The spectrum when the thickness of the Cr layers  $t_{Cr} = 80 \text{ \AA}$  in the multilayered structure  $[V(10 \text{ \AA})/Cr(40 \text{ \AA})/Sn(2 \text{ \AA})/Cr(40 \text{ \AA})]_{\times 29}/V(10 \text{ \AA})$  shows a magnetically split pattern. The hyperfine field has a Gaussian-like distribution with the maximum at the peak in the distribution around 10 T. In the case where the Sn layer is sandwiched by atomic Cr layers with antiparallel magnetization, a zero net transferred hyperfine field would be expected at the Sn nuclear sites. The large observed hyperfine field indicates that the magnetic moments of atomic Cr planes that are sandwiching the Sn layer are oriented in the same direction. The Gaussian-like feature proves that Cr magnetization is well ordered throughout the film plane with a definite value of the magnetic moment [12]. However, a minor single-line component of about 8% was detected. The hyperfine field for Sn dissolved in a Cr matrix is reported to be around 5.7 T at 295 K [10]. The enhanced value of the hyperfine field measured in the present work, as well as the hyperfine-field distribution, is similar to that reported for  $[Cr(40 \text{ \AA})/Sn(2 \text{ \AA})]$  multilayers except the minor component [11]. The enhanced hyperfine field is attributed to enhanced Cr magnetic moments at the Cr(001)/Sn interface. The V layers do not significantly influence the magnetic structure of Cr around the Cr/Sn interface when the Sn layer is located at 40 Å from the V/Cr interfaces. The intensity ratio of the sextet in the fitted spectrum shows that the Cr magnetic moments have

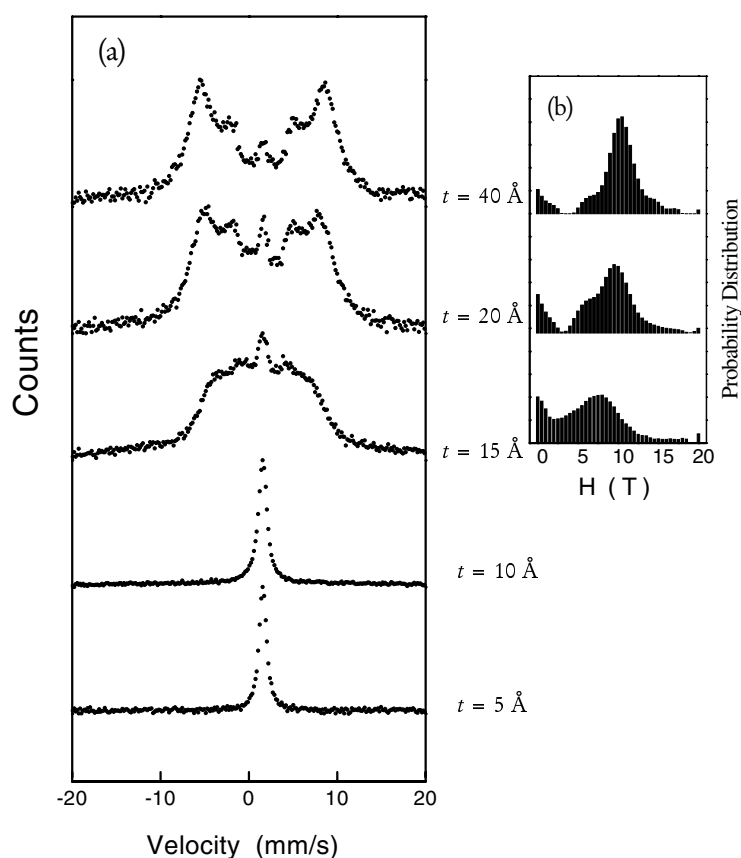


**Figure 3.** (a) Mössbauer spectra for  $[V(10 \text{ \AA})/Cr(t \text{ \AA})/Sn(2 \text{ \AA})/Cr(t \text{ \AA})]_{\times 29}/V(10 \text{ \AA})$  for  $t = 5, 10, 15, 20, 40 \text{ \AA}$  (from the bottom to the top) measured at 300 K; (b) the hyperfine-field distribution for  $t = 15, 20, 40 \text{ \AA}$ .

dominantly out-of-plane directions. The tendency of Cr magnetic moments to have a direction perpendicular to the film plane was reported for Ag/Cr multilayers, as investigated by PAC measurements [8].

The probability distribution of the hyperfine fields for the multilayer structure  $[V(10 \text{ \AA})/Cr(20 \text{ \AA})/Sn(2 \text{ \AA})/Cr(20 \text{ \AA})]_{\times 29}/V(10 \text{ \AA})$  shows a maximum at 9 T and has values at small fields larger than that expected from a Gaussian-like distribution. It is apparent that the V/Cr interfaces are affecting the magnetic structure of the Cr atomic layers at the Cr/Sn interface, where the Sn layer is located at 20 Å from the V/Cr interfaces, and leading to the observed distribution. The direction of the Cr magnetic moments, as inferred from the spectrum fit, does not change with decreasing Cr layer thickness.

As the Cr layer thickness  $t_{Cr}$  is reduced to 30 Å, the spectrum for the multilayer structure  $[V(10 \text{ \AA})/Cr(15 \text{ \AA})/Sn(2 \text{ \AA})/Cr(15 \text{ \AA})]_{\times 29}/V(10 \text{ \AA})$  shows a distribution around a smaller hyperfine field of 8 T with a distribution around the zero field superimposed on it. The decrease of the magnetic hyperfine fields at the Sn sites indicates a reduction of the magnetic moment of the Cr layers. The hyperfine field at the maximum in the distribution is larger than that detected for Sn dissolved in Cr, which confirms that the layered structure of V/Cr/Sn/Cr is well established.

The sample with a smaller Cr layer thickness, where  $t_{\text{Cr}} = 20 \text{ \AA}$ , with the multilayered structure  $[\text{V}(10 \text{ \AA})/\text{Cr}(10 \text{ \AA})/\text{Sn}(2 \text{ \AA})/\text{Cr}(10 \text{ \AA})]$ , shows a single-line pattern with a Lorentzian linewidth of  $1.2 \text{ mm s}^{-1}$  (the linewidth for non-magnetic Sn is  $\sim 1 \text{ mm s}^{-1}$ ). The V/Cr interface totally suppresses the Cr magnetic moments up to Cr atomic layers at the Cr/Sn interface when the Sn layer is located at  $10 \text{ \AA}$  from the V/Cr interfaces.

As there is no reference concerning the magnetic structure of Cr layers with a V/Cr interface in a multilayered structure, we consider the work reported for Cr–V alloys in the bulk state [1]. The Cr magnetization was reported to be strongly disturbed by adding V to a Cr matrix such that Cr single crystals with 0.5 at.% V are non-magnetic at room temperature and 4 at.% V totally suppresses the Cr magnetization down to 4.2 K.

The spectra measured for the samples deposited at room temperature give the same features as the samples deposited at  $200 \text{ }^\circ\text{C}$ . This feature of the hyperfine-field distribution together with the x-ray diffraction measurements suggests that intermixing between V and Cr, if it occurs, is limited and the change of the hyperfine field as a function of  $t_{\text{Cr}}$  is mainly due to a competition between the intrinsic magnetic order of Cr and the interfacial suppression effect at the V boundary layers. This conclusion is confirmed again by the Mössbauer measurements at 15 K.

*3.2.2. The magnetic state of Cr layers at low temperatures.* The Mössbauer spectra measured at 15 K are shown in figure 4. The hyperfine-field distribution for the multilayer structure  $[\text{V}(10 \text{ \AA})/\text{Cr}(40 \text{ \AA})/\text{Sn}(2 \text{ \AA})/\text{Cr}(40 \text{ \AA})]_{\times 29}/\text{V}(10 \text{ \AA})$  does not change significantly from that measured at room temperature, indicating that the Néel temperature of the Cr layers is higher than the bulk Néel temperature (the bulk Néel temperature was reported to be 311 K [1]). The hyperfine-field distribution shows two separate components: a major part around 11 T and a minor part of 8% around the zero field. A similar enhancement in the Néel temperature was reported for Cr thin films and multilayered structures [1–3]. The distribution for the  $[\text{V}(10 \text{ \AA})/\text{Cr}(20 \text{ \AA})/\text{Sn}(2 \text{ \AA})/\text{Cr}(20 \text{ \AA})]_{\times 29}/\text{V}(10 \text{ \AA})$  sample has a peak at 11 T and another at zero field of 14%. The magnetic structure, as inferred from the hyperfine-field distribution, does not significantly change as the temperature decreases from 300 K to 15 K, indicating that there is no reduction of the Néel temperature of the Cr layers. To distinguish the effect resulting from interdiffusion of V into the Cr matrix, we refer to the  $^{119}\text{Sn}$  Mössbauer measurements reported for  $\text{Cr}_{1-x}\text{V}_x$  alloy single crystals [10]. The Néel temperature was reported to decrease linearly with increasing V concentration and Cr becomes non-magnetic at 4.2 K for  $x \sim 4\%$ . Also the Cr magnetic moment and consequently the hyperfine field measured at 4.2 K were reported to decrease linearly with increasing V concentration. Therefore, the hyperfine field is expected to increase with decreasing temperature for the sample with V interdiffused in Cr with  $x < 4\%$ . At 4.2 K, the hyperfine-field value is expected to decrease as a function of V concentration. The spectrum collected for  $[\text{V}(10 \text{ \AA})/\text{Cr}(15 \text{ \AA})/\text{Sn}(2 \text{ \AA})/\text{Cr}(15 \text{ \AA})]$  shows a hyperfine-field distribution with a peak at 10.5 T and a minor single-line component. The large hyperfine fields detected for this sample lie in the range detected for Cr/Sn multilayers [11]. This indicates that there is no reduction of the Cr magnetic moment at low temperatures. Also the large value of the hyperfine fields, compared with those for Sn dissolved in Cr, confirms that the magnetic structure of Cr layers at the Cr/Sn interface is not disturbed and consequently the epitaxial multilayered structure is well established. The ratio of the single-line component does not decrease from that at room temperature. These observations confirm that the reduction of the magnetic hyperfine field at 300 K when  $t_{\text{Cr}} = 30 \text{ \AA}$  is not due to interdiffusion of V into Cr layers. The spectrum of  $[\text{V}(10 \text{ \AA})/\text{Cr}(10 \text{ \AA})/\text{Sn}(2 \text{ \AA})/\text{Cr}(10 \text{ \AA})]$  shows a hyperfine-field distribution around 5.5 T with a single line of 25%. The small values of the hyperfine fields indicate that Cr layers surrounding Sn have reduced magnetic moments

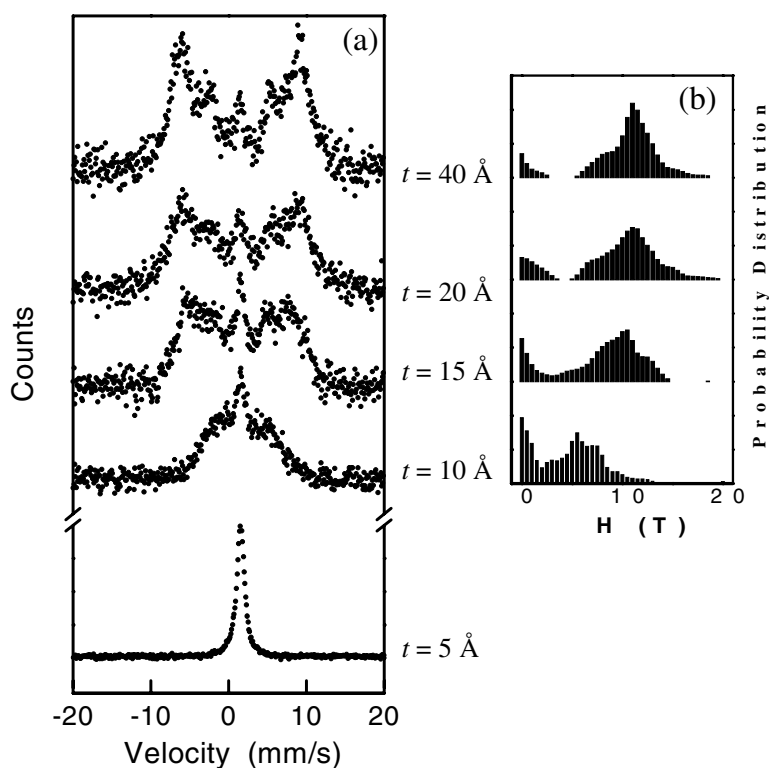


**Figure 4.** (a) Mössbauer spectra for  $[V(10 \text{ \AA})/Cr(t \text{ \AA})/Sn(2 \text{ \AA})/Cr(t \text{ \AA})]_{\times 29}/V(10 \text{ \AA})$  for  $t = 5, 10, 15, 20, 40 \text{ \AA}$  (from the bottom to the top) measured at 15 K; (b) the hyperfine-field distribution for  $t = 10, 15, 20, 40 \text{ \AA}$ .

at low temperatures. The spectrum of  $[V(10 \text{ \AA})/Cr(5 \text{ \AA})/Sn(2 \text{ \AA})/Cr(5 \text{ \AA})]$  shows a single line as observed at room temperature, indicating that V totally suppresses the Cr magnetic moment at the Cr/Sn interface, which is located about three atomic layers from the V/Cr interface. The change of the magnetization of the Cr layers between room temperature and 15 K indicates a change in the Néel temperature of the Cr. The reduction of the Néel temperature with decreasing Cr layer thickness is most probably due to a size effect of Cr layers at small thickness when bounded by V layers.

The electronic boundary conditions and the hybridization of the d-band electrons between V and Cr at an ideally sharp V/Cr interface are expected to reduce the Cr magnetic moment. At the real interfaces, additional effects are to be considered; the interface roughness or intermixing may suppress the Cr magnetic moments or disturb the Cr magnetic order in the region near the interface. Therefore, it seems reasonable that one of the interface effects or a combination of them will suppress the Cr magnetic moment and that Cr layers need a certain thickness to gain enough energy to overcome such suppression and attain the ordered magnetic structure with the bulk magnetic moment.

**3.2.3. The effect of the V/Cr interface on the Cr magnetization.** It was mentioned in the first section that when  $t_{Cr} = 80 \text{ \AA}$ , the suppression effect of the V/Cr interface on the Cr magnetic moment for  $[V(10 \text{ \AA})/Cr(40 \text{ \AA})/Sn(2 \text{ \AA})/Cr(40 \text{ \AA})]_{\times 29}/V(10 \text{ \AA})$  samples was totally



damped. Therefore the effect of a V/Cr interface on the Cr magnetization was investigated by changing the position of the Sn layer along the growth direction (figure 5). The multilayer structures were designated as  $[V(10 \text{ \AA})/Cr(80 - t \text{ \AA})/Sn(2 \text{ \AA})/Cr(t \text{ \AA})]_{\times 29}/V(10 \text{ \AA})$ , where  $t$  is the distance of the Sn monatomic layer from the upper interface (V deposited onto Cr). At  $t = 5 \text{ \AA}$ , which is about three atomic layers from the interface, the hyperfine field has a wide distribution ranging from zero field and a peak at 7 T. The Cr magnetic moment is expected to be totally suppressed at a V/Cr interface. The wide distribution of the hyperfine field indicates that the interface roughness disturbs the Cr magnetic order in the region near the V/Cr interface. The spectrum does not significantly change for the samples with the same designated thickness and deposited at room temperature, indicating that the interface structure is not especially remarkably influenced when the growth temperature is decreased from  $200 \text{ }^\circ\text{C}$  to room temperature. As the distance from the interface increases to  $10 \text{ \AA}$ , the hyperfine fields show a narrower distribution with a peak at 8.5 T. The variation in the hyperfine

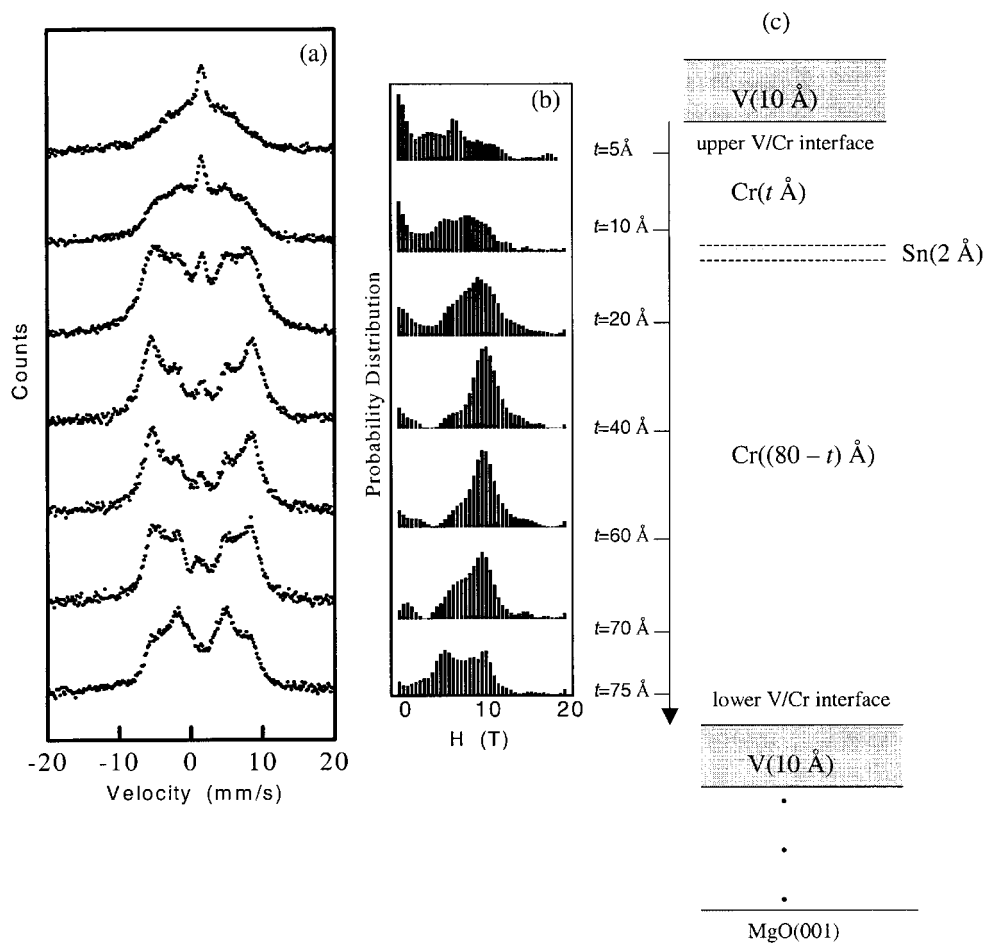


**Figure 5.** (a) Mössbauer spectra for  $[V(10 \text{ \AA})/Cr(80 - t \text{ \AA})/Sn(2 \text{ \AA})/Cr(t \text{ \AA})]_{\times 29}/V(10 \text{ \AA})$  for  $t = 5, 10, 20, 40, 60, 70, 75 \text{ \AA}$  (from the top to the bottom) measured at 300 K; (b) the hyperfine-field distribution for  $t = 5, 10, 20, 40, 60, 70, 75 \text{ \AA}$ ; (c) a sketch of one period in the multilayer structure. The vertical scale shows the positions of the Sn layer through the Cr layer.

field indicates that Cr magnetic moments increase on going far from the V/Cr interface. At  $t = 20 \text{ \AA}$  in the multilayered structure  $[\text{V}(10 \text{ \AA})/\text{Cr}(60 \text{ \AA})/\text{Sn}(2 \text{ \AA})/\text{Cr}(20 \text{ \AA})]_{\times 29}/\text{V}(10 \text{ \AA})$ , the distance of the Sn layer from the lower interface is  $60 \text{ \AA}$  and it is thought to be far enough away not to disturb the magnetic structure of the Cr atomic layers contacting the Sn layer. The hyperfine fields for this sample have a distribution like that for the sample  $[\text{V}(10 \text{ \AA})/\text{Cr}(20 \text{ \AA})/\text{Sn}(2 \text{ \AA})/\text{Cr}(20 \text{ \AA})]_{\times 29}/\text{V}(10 \text{ \AA})$ , where the distance of the Sn layer from the lower interface is  $20 \text{ \AA}$ . The effects acting on the magnetization of the Cr contacting the Sn layer in these two samples look the same. As the Sn layer is  $20 \text{ \AA}$  from the upper interface for both samples, the effect observed in the hyperfine-field distribution is thought to be resulting from the upper V/Cr interface. As the Sn layer is nearing the centre and at  $t = 40 \text{ \AA}$ , the interface effect seems to be totally damped as discussed in section 3.2.1. For the sample with  $t = 60 \text{ \AA}$ , where the Sn layer is at  $20 \text{ \AA}$  from the lower interface, the hyperfine-field distribution is the same as that observed for  $t = 40 \text{ \AA}$ . This is evidence that Cr atomic layers have homogeneous ordered magnetic structure with a definite magnetic moment through the Cr layers as long as the interface suppression effect is recovered. At  $t = 70 \text{ \AA}$  and when the Cr/Sn interface is  $10 \text{ \AA}$  from the lower V/Cr interface, the probability distribution at small hyperfine fields is larger than that expected for a Gaussian-like distribution, indicating the lower V/Cr interface effect. At  $t = 75 \text{ \AA}$  and when the Sn layer is  $5 \text{ \AA}$  from the lower interface, the hyperfine field was distributed with one peak at  $10 \text{ T}$  and another peak at  $5 \text{ T}$ , indicating that Sn atoms are located at two different magnetic sites. The hyperfine-field distribution around  $10 \text{ T}$  indicates that the Cr environment around Sn is magnetically similar to that in the middle of the Cr layers when the Sn layer is  $40 \text{ \AA}$  from the V/Cr interface. The hyperfine-field distribution around  $5 \text{ T}$  indicates the reduction of the Cr magnetic moment compared with its value at larger distance from the V/Cr interface. Since the nominal distance between V/Cr and Cr/Sn is  $5 \text{ \AA}$  and as the microscopic structure and topology are unknown for both interfaces, the origin of these two magnetic sites of Sn is not clear. Local strains at the lower interface may be responsible for stabilizing the magnetic order of Cr layers with non-zero magnetic moments. The ratio of the single-line component does not increase on changing the Sn layer position from  $40 \text{ \AA}$  to  $5 \text{ \AA}$  from the lower interface. Theoretical investigations of the V/Cr multilayer system show that Cr has a reduced magnetic moment near a V/Cr interface [14].

The hyperfine field measured when the Sn layer was set near the lower interface (Cr deposited onto V) has different features from that for the Sn layer set near the upper interface. As the interface effect would be dependent on the interface structure, these features indicate different structures of the two interfaces. The V/Cr interface effect is damped at a smaller distance from the lower interface than from the upper interface. Also the ratio of the single-line component decreases on going away from the upper one. Limited intermixing between V and Cr at the upper interface as V is deposited onto Cr or structural defects in Cr when it grows onto Sn would affect the V/Cr upper interface structure at small Cr thickness and lead to the different structures of the V/Cr interfaces.

To examine the magnetic order when Cr has reduced magnetic moments, as has been observed for  $t_{\text{Cr}} = 30 \text{ \AA}$ , another multilayered structure which is designated as  $[\text{V}(10 \text{ \AA})/\text{Cr}(10 \text{ \AA})/\text{Sn}(2 \text{ \AA})/\text{Cr}(20 \text{ \AA})]_{\times 29}/\text{V}(10 \text{ \AA})$  was investigated (figure 6). In this sample, the Sn layer is  $20 \text{ \AA}$  from the upper interface and  $10 \text{ \AA}$  from the lower one. At these distances, both interfaces are thought to be still affecting the Cr magnetic structure. The spectrum reveals a distribution with a reduced hyperfine field of  $8 \text{ T}$  at the peak. This distribution does not change especially remarkably from that of  $[\text{V}(10 \text{ \AA})/\text{Cr}(15 \text{ \AA})/\text{Sn}(2 \text{ \AA})/\text{Cr}(15 \text{ \AA})]_{\times 29}/\text{V}(10 \text{ \AA})$ , indicating that Cr orders with a reduced magnetic moment when the thickness of the Cr layer between V layers is  $30 \text{ \AA}$ .

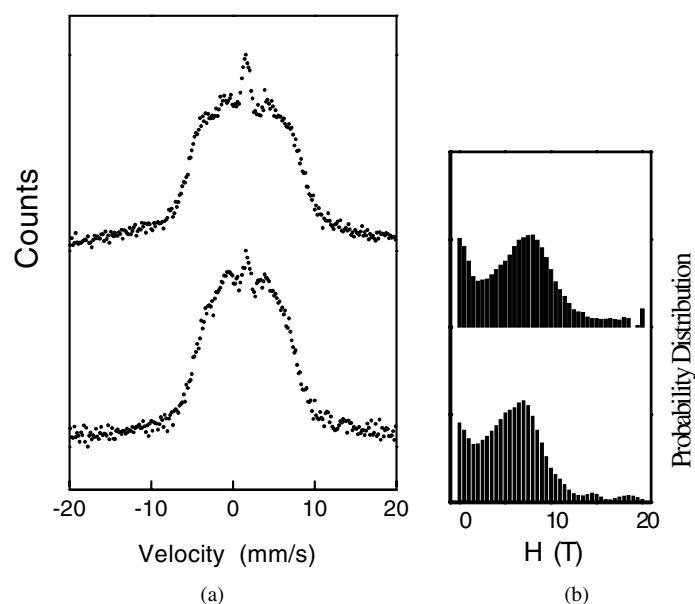


**Figure 6.** (a) Mössbauer spectra measured at 300 K for the two multilayer structures with the formulae  $[V(10 \text{ \AA})/Cr(15 \text{ \AA})/Sn(2 \text{ \AA})/Cr(15 \text{ \AA})]_{\times 29}/V(10 \text{ \AA})$  (upper set of data) and  $[V(10 \text{ \AA})/Cr(10 \text{ \AA})/Sn(2 \text{ \AA})/Cr(10 \text{ \AA})]_{\times 29}/V(20 \text{ \AA})$  (lower set of data); (b) the hyperfine-field distribution for the multilayer structures  $[V(10 \text{ \AA})/Cr(15 \text{ \AA})/Sn(2 \text{ \AA})/Cr(15 \text{ \AA})]_{\times 29}/V(10 \text{ \AA})$  (upper set of data) and  $[V(10 \text{ \AA})/Cr(10 \text{ \AA})/Sn(2 \text{ \AA})/Cr(20 \text{ \AA})]_{\times 29}/V(10 \text{ \AA})$  (lower set of data).

#### 4. Conclusions

Epitaxial V/Cr/Sn/Cr multilayered structures were grown at room temperature and 200 °C. The structural characterization through x-ray diffraction and Mössbauer spectroscopy shows that the magnetic structure does not change on changing the deposition temperature. The Mössbauer measurements performed at room temperature show a reduction of the Cr magnetic moment as the thickness of the Cr layer confined between V layers decreases below 40 Å and the Cr layers are non-magnetic at 20 Å. The Mössbauer measurements performed at 15 K show that Cr atomic layers around a Sn layer have ordered magnetic structure with no reduction of the magnetic moment when the Cr thickness is equal to or larger than 30 Å in the multilayered structures investigated. As the thickness decreases to 20 Å, the Cr layers have a reduced magnetic moment and the Cr layer with thickness 10 Å is non-magnetic. The Néel temperature when the Cr layer thickness is 40 Å is higher than the bulk Néel temperature. The change of the magnetization with decreasing temperature indicates the reduction of the Néel temperature with Cr layer thickness decreasing from 40 to 20 Å. The change of the Cr magnetic structure is most probably due to a Cr size effect and the boundary conditions at the V/Cr interface.

#### Acknowledgments

The authors thank Dr N Hosoi, Dr T Oguchi and Dr K Hirai for fruitful discussions during the course of this work. This work was partially supported by a Grant-in-aid for Creative Basic Research from Monbusho.

## References

- [1] Fawcett E 1988 *Rev. Mod. Phys.* **60** 209
- [2] Zabel H 1999 *J. Phys.: Condens. Matter* **11** 9303
- [3] Pierce D T, Unguris J, Celotta R J and Stiles M D 1999 *J. Magn. Magn. Mater.* **200** 290
- [4] Niklasson A M N, Johansson B and Nordstrom L 1999 *Phys. Rev. Lett.* **82** 4544  
Niklasson A M N 1998 *PhD Thesis* Uppsala University
- [5] Fishman R S and Shi Zhu-Pei 1999 *Phys. Rev. B* **59** 13 849
- [6] Slonczewski J C 1995 *J. Magn. Magn. Mater.* **121** 330
- [7] Stoeffler D and Gautier F 1991 *Phys. Rev. B* **44** 10 389
- [8] Demuyneck S, Meersschaut J, Dekoster J, Swinen B, Moons R, Vantomme A, Cottenier S and Rots M 1998 *Phys. Rev. Lett.* **81** 2562
- [9] Fullerton E E, Bader S D and Robertson J L 1996 *Phys. Rev. Lett.* **77** 1387
- [10] Dubiel S M, Cieslak J and Wagner F E 1996 *Phys. Rev. B* **53** 268  
Dubiel S M 1993 *J. Magn. Magn. Mater.* **124** 31
- [11] Mibu K, Tanaka S and Shinjo T 1998 *J. Phys. Soc. Japan* **67** 2633
- [12] Mibu K, Almokhtar M, Tanaka S, Nakanishi A, Kobayashi T and Shinjo T 2000 *Phys. Rev. Lett.* **84** 2243
- [13] Fukumura K, Nakanishi A, Kobayashi T and Isozumi Y 1994 *Nucl. Instrum. Methods Phys. Res. B* **86** 387
- [14] Hirai K 2000 unpublished